Biogeosciences Discuss., 11, 14097–14132, 2014
www.biogeosciences-discuss.net/11/14097/2014/
doi:10.5194/bgd-11-14097-2014

Biogeosciences Discussions
Open Access

Origin and fate of particulate and dissolved organic matter in a naturally iron-fertilized region of the Southern Ocean

L. Tremblay[1], J. Caparros[2,3], K. Leblanc[4], and I. Obernosterer[2,3]

[1]Department of Chemistry and Biochemistry, Université de Moncton, Moncton, NB, E1A 3E9, Canada
[2]CNRS, UMR 7621, Laboratoire d'Océanographie Microbienne, Observatoire Océanologique, 66650 Banyuls/mer, France
[3]Sorbonne Universités, UPMC Univ Paris 06, UMR 7621, Laboratoire d'Océanographie Microbienne, Observatoire Océanologique, 66650 Banyuls/mer, France
[4]Aix Marseille Université CNRS, Université de Toulon, IRD, Mediterranean Institute of Oceanography (MIO), UM 110, 13288, Marseille, France

Received: 3 September 2014 – Accepted: 17 September 2014 – Published: 2 October 2014

Correspondence to: L. Tremblay (luc.tremblay@umoncton.ca)

Published by Copernicus Publications on behalf of the European Geosciences Union.

Abstract

Natural iron fertilization of high-nutrient low-chlorophyll (HNLC) waters induces annually occurring spring phytoplankton blooms off Kerguelen Islands (Southern Ocean). To examine the origin and fate of particulate and dissolved organic matter (POM and DOM), D- and L-amino acids (AA) were quantified at bloom and HNLC stations. Total hydrolysable AA accounted for 21–25 % of surface particulate organic carbon (%POC_{AA}) at the bloom sites, but for 10 % at the HNLC site. A marked decrease in %POC_{AA} with depth was observed at the most productive stations leading to values between 3 and 5 % below 300 m depth. AA contributed to only 0.9–4.4 % of dissolved organic carbon (%DOC_{AA}) at all stations. The only consistent vertical trend was observed at the most productive station (A3-2) where %DOC_{AA} decreased from ~ 2 % in the surface waters to 0.9 % near 300 m. These AA yields and other markers revealed that POM and DOM were more rapidly altered or mineralized at the bloom sites compared to the HNLC site. Different molecular markers indicated that POM mostly originated from diatoms and bacteria. The estimated average proportion of POM from intact phytoplankton cells in surface waters was 45 % at the bloom station A3-2, but 14 % at the HNLC site. Estimates based on D-AA yields indicated that ~ 15 % of POM and ~ 30 % of DOM was of bacterial origin (cells and cell fragments) at all stations. Surprisingly, the DOM in HNLC waters appeared less altered than the DOM from the bloom, had slightly higher dissolved AA concentrations, and showed no sign of alteration within the water column. Unfavorable conditions for bacterial degradation in HNLC regions can explain these findings. In contrast, large inputs of labile organic molecules and iron, likely stimulate the degradation of organic matter (priming effect) and the production of more recalcitrant DOM (microbial carbon pump) during iron-fertilized blooms.

BGD
11, 14097–14132, 2014

1 Introduction

The Southern Ocean plays a key role in the global carbon cycle because it represents an important physical and biological CO_2 sink (Le Quéré et al., 2007). The magnitude of the biological contribution to the CO_2 sink is driven by primary productivity and the fate of the organic matter (OM) produced. It was univocally shown that iron controls primary production in the Southern Ocean, the largest high-nutrient low-chlorophyll (HNLC) ocean (Boyd et al., 2007). The extent to which biological degradation of particulate (POM) and dissolved organic matter (DOM) affect their potential export to depth and preservation is far from understood (Ebersbach and Trull, 2008).

Natural iron fertilization induces intense phytoplankton blooms in spring, especially around the Kerguelen islands (Blain et al., 2007). Blooms induced by natural iron fertilization likely represent major events for heterotrophic bacteria which are reported to be limited by carbon in the HNLC Southern Ocean (Church et al., 2000). Indeed, pronounced responses of heterotrophic bacteria are reported from natural iron fertilization studies (Zubkov et al., 2007; Christaki et al., 2008, 2014). Rapid bacterial mineralization of $\sim 45\,\%$ of the primary production was observed during the decline of the spring phytoplankton bloom above the Kerguelen Plateau (Obernosterer et al., 2008). Furthermore, the efficiency of the carbon export, defined as the ratio of particulate organic carbon (POC) in deep waters to primary production, was about two times lower above the Kerguelen Plateau than in HNLC waters (Savoye et al., 2008). These findings suggest that the POM produced during the bloom is relatively labile, and rapidly turned over. Although DOM production is an essential step during bacterial mineralization, the effect of iron fertilization on the concentration and reactivity of DOM has been far less studied.

To better understand to role of the Southern Ocean in the cycles of carbon and other vital elements, such as nitrogen, it is important to study the origin and fate of its OM in regions having contrasting conditions and productivities. To do so, molecular level analyses of POM and DOM provide unique and valuable pieces of information. Amino

BGD
11, 14097–14132, 2014

acid enantiomers (L- and D-AA) are among the few markers that can be analyzed in bulk seawater at ambient concentrations and provide numerous indicators on OM origin and fate (e.g., Kaiser and Benner, 2008; Dittmar et al., 2009). AA contain most of the nitrogen in living organisms and are important constituents of detrital POM and DOM (Cowie and Hedges, 1992). While L-AA are ubiquitous (e.g., all proteins), D-AA are only produced in important proportions in bacteria (Asano and Lübbehüsen, 2000).

AA are generally selectively utilized by heterotrophic organisms compared to bulk OM. As a result, the proportions of bulk carbon and nitrogen in the form of AA, or AA yields, decrease with time and are useful indicators of POM and DOM alteration state (Cowie and Hedges, 1994; Davis et al., 2009). Other independent diagenetic markers are the molar percentage of D-AA vs. total hydrolysable AA (THAA) (Tremblay and Benner, 2009) and the degradation index (DI) calculated based on the relative distribution of individual AA (Dauwe et al., 1999; Peter et al., 2012). An increase in mol% D-AA during degradation is attributed to the bacterial contribution of D-AA to the OM and to a lower degradation rate of the bacterial biomolecules rich in D-AA compared to proteins having only L-AA (Nagata et al., 2003). During degradation some AA are selectively degraded (the others are selectively preserved) and these changes reduce the DI value. AA yields are known to be more sensitive to the first alterations of the OM compared to mol% D-AA and DI which require more intense alterations before showing consistent changes (Davis et al., 2009; Bourgoin and Tremblay, 2010).

C- and N-normalized yields of individual D-AA (e.g., D-alanine) were shown to have a similar dynamic as bulk bacterial C and N, respectively (Tremblay and Benner, 2006; Kaiser and Benner, 2008). Thus, these yields can be used to estimate the contribution of bacteria (from intact cells and cell fragments or detritus) to POM and DOM. In addition, plots of the sum of serine and threonine vs. the ratio aspartic acid/glycine have been previously utilized to discriminate different carbon sources, specifically diatoms, coccolithophores and bacteria (Ittekkot et al., 1984; Gupta and Kawahata, 2000; Salter et al., 2010).

BGD
11, 14097–14132, 2014

The objective of this work was to evaluate the origin and fate of the OM produced during spring phytoplankton blooms in the naturally iron fertilized Southern Ocean. To do so, bulk and AA enantiomeric analyses were done on unfiltered and filtered waters collected at different bloom sites and in HNLC waters during the KEOPS2 (KErguelen Ocean and Plateau compared Study 2) expedition. This work provides a detailed description of OM characteristics and new evidences on the distinct fates of the OM from naturally iron fertilized regions.

2 Materials and methods

2.1 Site description and sampling

Among the sampling sites visited during the KEOPS2 campaign in October and November 2011, five stations were selected for the present study (Table 1) (map available in Blain et al., 2014). Station R-2 (bottom depth = 2532 m) was located in a HNLC region outside the western boundary of the Kerguelen Plateau. In contrast, Station A3-2 (bottom depth = 527 m) was in the center of the phytoplankton bloom that occurs annually above the Kerguelen Plateau. Stations E-1 (bottom depth = 2056 m) and E-5 (bottom depth = 1920 m) were located in offshore waters within a stationary meander South of the Polar Front and these stations were sampled in a quasi-Lagrangian manner before (E-1) and during the bloom (E-5). TEW-2 is a shallow station (total depth = 85 m) above the eastern continental shelf of Kerguelen Island and it is characterized by continental inputs and relatively high productivity. Sampling depths were selected to cover important features of water masses revealed by CTD profiling. The surface mixed layer depth was 105 m at Station R-2, 153 m at Station A3-2, 46 m at Station E-5, 72 m at Station E-1 and 40 m at Station TEW-2. Because of water quantity and time limitations, only the first 350 m of the water column were sampled at E-5.

Water samples for AA, dissolved organic carbon (DOC) and nitrogen (DON) analyses were collected using 10 L Teflon-lined Niskin-1010X bottles mounted on a 1018

BGD
11, 14097–14132, 2014

rosette system adapted for trace metal clean work (Bowie et al., 2014). Subsamples were transferred to 500 mL Schott glass bottles that were rinsed with acid (HCl, 10 %) and then ultrapure water before use. Part of each water sample was filtered through two combusted GF/F filters (0.7 µm nominal pore size, Whatman) using a Hamilton glass syringe and PTFE tubing. For AA analyses of the dissolved fraction, 20 mL of the GF/F filtered water were stored in HDPE bottles at −20 °C. For DOC analyses, 15 mL of the GF/F filtered water were acidified (H_3PO_4, final pH = 2) and stored in the dark in combusted and sealed glass ampoules. DON analyses were done with an aliquot of the GF/F filtered water that was stored poisoned (100 µL of $HgCl_2$; 4 g L^{-1}, working solution) in PTFE bottles (Blain et al., 2014). Total AA (dissolved and particulate) were determined in 20 mL of unfiltered water stored in HDPE bottles at −20 °C. The concentration of particulate AA was calculated by subtracting the AA concentration in filtered water from the total AA concentration.

Water samples for particulate organic carbon (POC) and nitrogen (PON) analyses were collected with regular 12 L Niskin bottles. 1 L of seawater was filtered on combusted GF/F filters, and the filters were stored in the dark until analyses (Lasbleiz et al., 2014). The sampling depths of these water samples did not always perfectly match the depths of the samples used for the other analyses. In these cases, the depths that were the closest to those shown on Table 1 were used for POC and PON.

2.2 Organic carbon and nitrogen analysis

DOC concentrations were measured on acidified aliquots using a Shimadzu TOC-VCP analyzer with a Pt catalyst at 680 °C (Benner and Strom, 1993). All DOC analyses were run in duplicate and 3–5 injections were done for each sample. Analytical precision was 0.2–1 % (CV). Reference materials (http://www.rsmas.miami.edu/groups/biogeochem/CRM.html) was injected every 15 samples to insure stable operating conditions. DON concentrations were determined after wet oxidation and calculated as the difference between total N concentration and the sum of inorganic N (i.e., nitrate, nitrite, ammonium) (Blain et al., 2014). Inorganic N was determined by the automated colorimetric

BGD
11, 14097–14132, 2014

technique on a Skalar autoanalyzer (Aminot et Kérouel, 2007). POC and PON analyses of particles on filters were done on an PerkinElmer 2400 CHN analyzer (Lasbleiz et al., 2014). The filter blank values for POC and PON corresponded to 1.27 µM ± 0.26 and 0.06 µM ± 0.02, respectively.

2.3 Amino acid analysis

AA enantiomers (L and D) and achiral AA were measured after liquid-phase acid hydrolysis and reversed-phase high performance liquid chromatography (HPLC) according to a newly developed procedure (Escoubeyrou and Tremblay, 2014). This procedure is similar to traditional ones, except that a high volume (100 µL) of undiluted samples is injected and a robust hybrid C-18 column is used. These changes increase the precision of the measurements while providing a more consistent separation.

Briefly, 366 µL of seawater (filtered or unfiltered) were transferred to an ampoule and mixed with 634 µL of HCl 30 % (Merck, Suprapur grade). Procedural blanks were also prepared with 634 µL of HCl 30 %. The ampoules were then vacuum sealed and placed at 110 °C for 20 h. After hydrolysis, 300 µL of hydrolysate (190 µL for blanks) were evaporated on a Genevac Personal Evaporator (EZ2+ HCl compatible). 150 µL of ultrapure water were then added and evaporated to remove remaining traces of HCl. Samples consisting of 110 µL of non-hydrolyzed seawater were also evaporated for the analysis of free AA. Samples and blanks were then dissolved in 120 µL of borate buffer (0.4 M, Merck, Suprapur) with a pH adjusted to 10 with NaOH 6 M (Merck, Suprapur). Strong vortex agitation and sonication were necessary to completely dissolve the dried residue. The vials were then centrifuged (4300 rpm, 5 min) to separate the flocculate formed in borate buffer.

HPLC analyses were performed on an Ultimate 3000 Dionex system equipped with an autosampler and a fluorescence detector (excitation at 335 nm, emission at 450 nm). The separation was done with a Phenomenex Gemini C18 column (250 mm × 4.6 mm, 5 µm, 110 Å) and a Security Guard column (4 mm × 3 mm). Automated precolumn derivatization with o-phthaldialdehyde (OPA) and N-isobutyryl-L-cysteine (IBLC, L-run)

BGD
11, 14097–14132, 2014

or with OPA and N-isobutyryl-D-cysteine (IBDC, D-run) was performed. 2 mg of OPA and 5 mg of IBLC or IBDC were dissolved in 200 µL of methanol and diluted with 1.8 mL of ultrapure water. 100 µL of sample or blank were derivatized with 10 µL of OPA/IBD(L)C reagents. 10 µL of S-Methyl-L-cysteine (SMC, 0.74 µM) were added to the reaction mixture as an internal standard. After a reaction time of 2 min at 8 °C, 100 µL of this mixture were injected. OPA/IBLC (run L) and OPA/IBDC (run D) were used alternatively for every sample and blank. The elution order of L-AA and D-AA is reversed during the second run, which increases the accuracy of peak identification and quantification (Brückner et al., 1994). The largest peak of the two runs was not considered because it may be caused by a coelution. The column temperature was maintained at 44 °C. A gradient of organic phase (93 % methanol, 7 % acetonitrile) and KH_2PO_4 aqueous solution (40 mM, pH 6.15) was used with a flow rate of 0.8 mL min^{-1} (Escoubeyrou and Tremblay, 2014).

Before injecting samples, blanks or standards, several analyses of borate buffer were performed to check the level of contamination from free AA. AA identification and quantification in unknown samples and blanks were achieved by comparing the retention times and peak areas with those of standard AA solutions. Coefficients of determination of calibration curves were always between 0.99 and 1.0. Standard solutions contained 23 AA: L- and D-aspartic acid (L/D-Asp), L- and D-glutamic acid (L/D-Glu), L- and D-serine (L/D-Ser), L- and D-alanine (L/D-Ala), L- and D-valine (L/D-Val), L- and D-leucine (L/D-Leu), L-threonine (L-Thr), glycine (Gly), L-arginine (L-Arg), L-isoleucine (L-Ileu), L-phenylalanine (L-Phe), L-lysine (L-Lys), L-histidine (L-His), L-tyrosine (L-Tyr), L-methionine (L-Met), γ-aminobutyric acid (Gaba), and β-alanine (BAla).

Peak areas of AA measured in blanks were subtracted from those in samples. The borate buffer solution was used as the blank for the quantification of free AA. Individual AA concentrations in injected samples were then calculated using the slope of calibration curve of each AA. The average racemization rates of individual free and protein AA occurring during hydrolysis and measured by Kaiser and Benner (2005) were used to correct the concentrations of chiral AA. Asp and Glu peaks included the contribution of

BGD
11, 14097–14132, 2014

L-glutamine (Gln) and L-asparagine (Asn), respectively, that were deaminated during hydrolysis. They were thus identified by Asx and Glx.

Particulate THAA were quantified by the difference between the peak areas obtained with unfiltered and filtered hydrolyzed samples. The chromatograms of filtered samples were used to quantify dissolved AA, which are the sum of free and dissolved combined AA. Dissolved combined THAA can be determined by the difference between the peak areas obtained with filtered hydrolyzed and non-hydrolyzed samples. The limits of detection were 0.007–3.57 nM depending on the AA (Escoubeyrou and Tremblay, 2014). Most particulate AA (determined by difference) were near their limit of detection in samples having low POC concentrations. This increases the uncertainty of particulate AA, POC and PON values in these samples.

2.4 Chlorophyll analysis

Concentrations of chlorophyll *a* were determined by HPLC following the protocol of Van Heukelem and Thomas (2001) modified by Ras et al. (2008). Seawater samples (1 to 2.23 L) were filtered on 25 mm GF/F filters (Whatman) which were then stored in cryotubes in liquid nitrogen until further processing in the home lab as described in detail in Lasbleiz et al. (2014).

3 Results

3.1 Organic carbon and nitrogen

Striking differences in OM concentrations and compositions were observed between stations (Table 1). As expected, Station R-2 located in the HNLC region exhibited the lowest chlorophyll *a* ($< 0.32\,\mu g\,L^{-1}$) and POC concentrations (1.5–7.8 µM) compared to the other stations for similar depths. The highest concentrations of chlorophyll *a* (up to $2.4\,\mu g\,L^{-1}$) and POC (up to 14.8 µM) were observed in the mixed layer at Station A3-2. Station E-1, sampled before the bloom, had relatively low POC concentrations

BGD
11, 14097–14132, 2014

in its surface waters (7.7 µM at 20 m). 19 days later, the POC concentrations increased to 11 µM at E-5. There was a marked decrease in POC concentrations with depth, especially at station A3-2 showing a 7.4-fold decrease. The lowest POC concentrations, 1.5–3 µM, were measured below 210 m.

DOC represented 78 % (surface water of A3-2) to 97 % (deep water of R-2) of total organic carbon (Table 1). Despite a slight decreasing trend with depth at all stations, DOC concentrations were much less variable than those of POC. The highest concentrations (51–52 µM) were measured in the surface waters of Station A3-2, the bloom site above the plateau. The lowest concentration (44 µM) was found in the deep waters of the less productive Station R-2.

PON and DON concentrations also varied with location and depth (Table 1). They generally followed the same trends as their carbon counterparts, although not always to the same extent as indicated by the POC/PON and DOC/DON ratios in representative samples (Fig. 1). A preferential degradation of N-rich molecules in particles lead to a general increase in POC/PON ratios with depth (Fig. 1a). As expected, the particles in the surface waters of the bloom at stations A3-2 and E-5 were enriched in N. In contrast, the HNLC region (Station R-2) had more N-poor particles (Fig. 1a) and 2 to 3.5 times lower PON concentrations (Table 1). DON concentrations varied from 7.6 µM at station TEW-2 to 2.7 µM in the deep waters of Station A3-2. Station A3-2 was the only site where DON concentrations decreased (Table 1) and DOC/DON ratios increased with depth (Fig. 1b). This indicates that N-rich dissolved organic molecules at Station A3-2 are more easily or rapidly degraded than those from the other stations.

3.2 Amino acid concentrations

Table 1 presents AA concentrations measured in the particulate and dissolved fractions. As expected, the most productive stations (A3-2, E-5, and TEW-2) had the highest concentrations of particulate THAA. The water collected at the surface of these stations contained between 539 and 821 nM of particulate THAA, while concentrations were 162–223 nM in the surface waters of stations R-2 and E-1. Though deep waters

BGD
11, 14097–14132, 2014

contained less particulate THAA than surface waters at all stations, the decrease with depth was much faster at the bloom sites. These concentrations dropped by a factor 20 and 37 at stations E-5 and A3-2, respectively, but only by a factor ∼ 5 at stations R-2 and E-1. At stations R-2 and E-1, particulate THAA concentrations were maximal in the subsurface layer (40–100 m), and not at the surface like for bloom locations. This suggests a production of particulate THAA in subsurface or a localized removal mechanism (e.g., photo-oxidation) in the first meters of the water column at stations R-2 and E-1.

In contrast to particulate THAA, concentrations of dissolved AA (combined and free AA) were generally higher at the less productive locations (R-2 and E-1; up to 495 nM) than at the bloom sites (A3-2 and E-5; 128–292 nM) for similar depths (Table 1). The shallow Station TEW-2 also had high concentrations (403–489 nM). However, a greater proportion of dissolved AA were free AA at the surface of stations A3-2 and E-5 compared to Station R-2 (13.5–23.6 % vs. 11.3 %, Table 1). Station A3-2 exhibited the highest concentrations of free AA (52–69 nM, Table 1), but lower dissolved combined AA (e.g., in proteins and peptides) concentrations than Station R-2.

Concentrations of total dissolved AA decreased with depth, by a factor 1.4 to 2.2 (Table 1), except in the shallow water column at Station TEW-2. The decrease in free AA was more important (factor 3.4–5.2). These trends were more pronounced at the bloom Station A3-2, but were not as marked as for particulate THAA.

3.3 Amino acid yields and diagenetic markers

AA are the most abundant organic N-molecules in nature. We thus expect to see similar trends in the proportions of N and of THAA in POM as indicated by POC/PON (Fig. 1a) and $\%POC_{AA}$ (Fig. 2a), respectively. Both parameters indicated higher proportions of N-molecules in POM at stations A3-2 and E-5 and a decrease in these proportions with depth at all stations. The decrease in $\%POC_{AA}$ was particularly marked at stations A3-2 and E-5 where THAA accounted for 22–25 % of POC in the surface waters, but only for 4.2–4.9 % below 300 m (Fig. 2a). Particulate THAA accounted for 30–51 % of

BGD
11, 14097–14132, 2014

PON in the surface of the more productive stations and for 27 % at Stations R-2, and these proportions decreased with depth at all stations, especially at Station A3-2 (not shown). The degradation of particulate THAA was thus more rapid than that of other N-molecules.

Dissolved AA contributed to only 0.86–2.7 % of DOC at stations R-2, A3-2 and E-5 (Fig. 2b). $\%DOC_{AA}$ were slightly higher in the surface sample of stations E-1 and TEW-2 (2.4–4.4 %, E-1 and TEW-2 data not shown). The only consistent vertical trend was observed at Station A3-2 where $\%DOC_{AA}$ decreased with depth from ∼ 2 to 0.86 %. This suggests a preferential removal of dissolved AA with depth at this bloom station. This trend is not observed or is less marked at the other stations. Dissolved AA contributed to 2.3–8 % of DON with no trend according to station or depth (not shown).

During degradation, the mol% D-AA should increase and the DI should decrease. These markers indicated that POM from Station R-2 was more altered than the POM from the other stations (Figs. 3a and 4a), in agreement with its lower N and THAA contents. However, mol% D-AA and DI did not show consistent trends with depth, except for mol% D-AA at Station R-2 (Fig. 3a) and for DI in deep waters only (Fig. 4a). Clearly, these markers were not as sensitive, or effective, as $\%POC_{AA}$ (or POC/PON) for tracking POM degradation with depth in the present study. In the dissolved fraction, mol% D-AA and DI values suggest, once again, that DOM from Station R-2 was less altered (Figs. 3b and 4b). However, no sign of alteration with depth was observed at this station. In fact, the only station showing a clear increase of DOM alteration state with depth was, once again, A3-2 (Figs. 3b and 4b). From 40 to 300 m, mol%D-AA went from 5 to 10 % and the DI from 0.5 to −1.7 in DOM. The increase in mol%D-AA in total OM (POM and DOM) with depth at Station A3-2 was even more important (from ∼ 2 to 8 %, not shown).

3.4 Markers of organic matter origin

The average values of Ser + Thr and Asp/Gly found in diatoms, coccolithophores and bacteria (Muller et al., 1986; Cowie and Hedges, 1992) are presented in Fig. 5, along

BGD
11, 14097–14132, 2014

with the values measured here at stations A3-2 and E-5. All the data points for POM (open circles) are near averages values (open boxes) found in diatoms or between those of diatoms and bacteria suggesting that the POM mostly originated from diatoms and bacteria. Except for one data point at each of the other stations having Asp/Gly over 1.5, the same conclusion can be stated for the other studied locations (not shown). No trend with depth was observed for Ser + Thr, but Asp/Gly generally decreased with depth (not shown). Gly is known to be selectively preserved during POM degradation (Dauwe et al., 1999). Changes in the composition of AA during degradation (e.g., microbial) is certainly responsible for the lower Ser + Thr and Asp/Gly values measured in DOM (Fig. 5).

Chlorophyll *a* and D-AA can be used to estimate the proportions of organic matter associated with phytoplankton (cells) and bacteria (cells and detritus), respectively. The ratios of chlorophyll *a* to POC concentrations (concentrations in Table 1) at stations A3-2 and E-5 is more than twice those measured in the HNLC Station R-2. This difference can be due to a higher proportion of phytoplanktonic cells in the POM from the bloom and/or to lower intracellular chlorophyll content in the phytoplankton of the HNLC region. Assuming that diatom dominated phytoplankton communities have 40 times more carbon than chlorophyll *a* on a per cell basis (Sathyendranath et al., 2009), calculations indicated that phytoplankton biomass could account for 14 % of POC in the surface water of Station R-2, but for 35–63 % in the surface waters of the other stations (not shown), except at 30 m of TEW-2 where 81 % was calculated. Estimates were much lower in the deep waters, with 2.3 % calculated at Station R-2 (200 m) and 8.3 % at Station A3-2 (300 m). This approach takes mostly into account phytoplankton cells (vs. altered fragments) considering that a rapid decrease in chlorophyll *a* content is expected in phytoplankton detritus.

D-AA can be used to estimate the proportions of OM coming from bacterial cells and altered cell fragments or detritus. D-Asx yields varied from < 2 to 31.7 nmol mg^{-1} POC and D-Glx yields varied from < 2 to 18.1 nmol mg^{-1} POC (Table 2). In both cases, the highest values were measured above 200 m in the water columns. D-Ala yields were

BGD
11, 14097–14132, 2014

highly variable, < 2 to 68.8 nmol mg^{-1} POC with no clear trend with depth. The sample collected at 200 m at Station R-2 exhibited relatively high values for each D-Asx, D-Glx and D-Ala (31.7, 18.1 and 53.7 nmol mg^{-1} POC, respectively) suggesting a greater contribution of bacteria to POC in this sample. Average yields reported in cultured marine bacteria (Kaiser and Benner, 2008) represent 15, 48 and 50 nmol mg^{-1} POC for D-Asx, D-Glx and D-Ala, respectively (Table 2). Comparisons between these values and those measured here in POM suggest that a significant, although variable, fraction of POC can be from bacteria. For instance, at Station A3-2, where higher POC concentrations increase estimation accuracy and precision, D-Glx and D-Ala yields suggest that ~ 5 to 20 % of the POC was from bacteria. However, the lack of correlations, or consistent trends, between the D-AA biomarkers and the large ranges of D-AA yields in POM (and bacteria) makes it difficult to provide estimates of the percentages of POM coming from bacteria based on this approach.

D-AA yields in the dissolved fraction were much more consistent (Table 2). Figure 6 shows average values measured in DOM produced by bacteria (Kaiser and Benner, 2008) and in DOM from surface (0–120 m) and deep waters (> 120 m) at stations impacted (A3-2 + E-5) or not (R-2 + E-1) by the bloom. D-Asx and D-Ala yields suggest that 16.5–35 % of this DOC is from bacteria, with the lowest estimates found in the deep waters of stations R-2 and E-1. Similar trends, but lower estimates (10.4–17.5 %) were obtained when D-Glx yields are used. D-Glx yields in bacterial DOM are highly variable (Kaiser and Benner, 2008), and the reference average value used here might be higher than that of the bacterial DOM produced in the studied waters.

4 Discussion

4.1 Amino acids in the Southern Ocean

This study presents the first detailed quantification of particulate and dissolved AA in the Southern Ocean. The measured concentrations, yields, and relative distributions

BGD
11, 14097–14132, 2014

of AA in POM and DOM were in the range of values previously found in other marine waters, from the open equatorial Pacific (Lee et al., 2000) to the coastal waters of the Arctic (Dittmar et al., 2001) and Northern Atlantic oceans (Bourgoin and Tremblay, 2010). THAA represented between 21 and 25 % of POC in the surface waters of bloom sites which is close to the 27 % measured in suspended particles at the chlorophyll maximum depth in the equatorial Pacific (Lee et al., 2000). Such high values are expected when protein-rich plankton represents an important part of POM (see 4.2 below) (Cowie and Hedges, 1992, 1994). Concentrations of chlorophyll *a* and POM were highest in the surface water of the bloom Station A3-2, consistent with a greater production of biomass induced by iron inputs. In contrast, THAA represented 10 % of POC at Station R-2 which is expected in more altered POM (Cowie and Hedges, 1994).

A particularity of the Southern Ocean surface waters are the lower DOC concentrations compared to other oceans (i.e., ~ 50 µM vs. 70–80 µM) (Hansell, 2013). Here, AA accounted for only 0.9–4.4 % of DOC, which is in the range of values found in other regions (Benner, 2002; Bourgoin and Tremblay, 2010). However, AA yields in the DOC of HNLC surface water (2.7 %) were about twice that measured in the oligotrophic North Pacific near Hawaii (Kaiser and Benner, 2008). This suggests more favorable conditions for AA accumulation/preservation in the HNLC of the Southern Ocean.

4.2 Origin and fate of POM

Molecular AA markers (i.e., Ser + Thr, Asp/Gly and D-AA yields) indicated, at least qualitatively, that the POM at the bloom sites mostly originated from diatoms and bacteria. Different approaches was used to estimate the proportion of each of these components of the plankton community. Pigment analysis and microscopic observations confirmed that diatoms were abundant in surface waters of the bloom sites (Lasbleiz et al., 2014). Species-specific biovolume determination in the euphotic layer (between the surface and 0.01 % PAR) revealed that diatoms accounted, on average, for 44 % of POC at Station A3-2, while their contribution to POC was only 5 % at the HNLC site (Lasbleiz, 2014) (Table 3). These observations are consistent with the present esti-

BGD
11, 14097–14132, 2014

mates based on chlorophyll *a* concentrations, indicating that phytoplankton cells could account on average for 45 % of POC in the surface waters of Station A3-2, but 14 % of POC in the surface waters of Station R-2 (Table 3). The lower proportion of diatoms among the phytoplankton community at Station R-2 is in agreement with direct observations (Lasbleiz et al., 2014). These estimates were 5–7 times lower below 200 m at both locations (Table 3). In deep waters, the phytoplankton contribution to POC is thus likely dominated by detrital material (vs. intact cells). Laurenceau et al. (2014) used microscopic observations of material collected in gel traps and estimated that phytodetrital aggregates represented 41 and 34 % of POC at stations A3-2 and R-2, respectively, in sinking particles collected at 210 m (Table 3). Both types of estimates show the same trend of a higher phytoplankton contribution at Station A3-2. The higher percent contribution obtained for the gel traps is most likely due to the fact that this approach considers both living and dead phytoplankton cells, and that particles defined as phytodetrital aggregates can contain POC from other origins (e.g., bacteria).

D-AA yields were used to estimate the proportion of POC from bacteria (cells and altered debris of bacteria). However, some extreme and inconsistent values were measured in the present dataset. Extreme values or the disagreement between D-AA yields are probably caused by the fact that yields in POM were calculated by difference between the chromatographic peaks measured in unfiltered and filtered water samples. In many samples, this difference was very small, because of the very low POM concentrations, increasing the uncertainty of these yields. Different dynamics between D-Asx, D-Glx et D-Ala in the studied POM could also explain inconsistent values. This appears to be the case at Station A3-2, where D-Glx and D-Ala markers were not always in agreement, despite the increased estimation accuracy and precision due to the higher POC concentrations. For instance, at 70 m at this site, estimates based on D-Glx and D-Ala were 19 and 5 %, respectively (not shown). Averages suggest that ~ 15 % of the POC originated from bacteria at all depths at Station A3-2 (Table 3, Bacteria total). Using the same approach and markers, Kaiser and Benner (2008) estimated that about

BGD
11, 14097–14132, 2014

25 % of POC were of bacterial origin in oligotrophic areas of the North Pacific and North Atlantic.

An independent approach, based on cell counts of autotrophic (unpublished data) and heterotrophic bacteria (Christaki et al., 2014) and conversion of cell counts to carbon units using 250 fg C cell^{-1} for autotrophic (Campbell et al., 1994) and 12.4 fg C cell^{-1} for heterotrophic bacteria (Fukuda et al., 1998), revealed that only 2–3 % of POC are accounted for by bacterial cells as determined by flow cytometry in the surface waters at Station A3-2 (Table 3, Bacteria biomass). However, there was a steady increase of this proportion with depth at Station A3-2, to up to 10 % at 300 m. When compared to the D-AA estimate of ~ 15 % of POC originating from bacteria, it appears that intact bacterial cells represent a small proportion (< 20 %) of the total bacterial contribution (living + detritus) in the surface water, which is in agreement with previous studies (e.g., White and Howes, 1994; Bourgoin and Tremblay, 2010). However, intact bacterial cells appear to dominate (67 %) the bacterial contribution in the deep waters at the bloom site. This increase in bacterial cell contribution with depth was not observed at the HNLC site where proportions fluctuated between 4–7 % of POC. Different trends have been reported in previous studies. As observed here at the bloom site, the proportion of POC as bacterial biomass increased with depth in the St-Lawrence Gulf (Bourgoin and Tremblay, 2010). This trend was caused by a depletion of bacterial POM with depth that was more intense than the decrease of bacterial biomass with depth. In contrast, Kawasaki et al. (2011) estimated that bacterial detritus represented a greater proportion of POC (vs. living bacterial biomass) at 100 m (~ 7 %) than at 5 m (~ 4.5 %) in an oligotrophic area of the North Pacific gyre. However, autotrophic bacteria accounted for ~ 13 % of their POC which was about 50 % of the total bacterial contribution (living + detritus). In the present study, autotrophic bacteria (*Synechococcus*) had low cell numbers (2–10 × 10^5 cells L^{-1}; data not shown). It thus appears that a high lability of bacterial detritus and a low proportion of autotrophic bacteria increase the relative proportion of living bacteria vs. bacterial detritus in POC in deep waters as in the present study (see below).

BGD
11, 14097–14132, 2014

A large fraction of the POM remains of unknown origin, especially in the HNLC site. This fraction could be mostly from detritus of various origins including zooplankton. Laurenceau et al. (2014) estimated that zooplankton fecal pellets represented on average 56 ± 19 % of POC flux below 110 m at the studied locations. These pellets contain materials from different origins including phytoplankton (Silver and Gowing, 1991).

The reactivity of POM was markedly higher at the bloom site A3-2 compared to the HNLC site, as revealed by a much more rapid decrease of POM and particulate THAA concentrations with depth. In addition, THAA yields in POM (%POC_{AA} and %PON_{AA}), reliable indicators of POM alteration or diagenetic state (Cowie and Hedges, 1994; Tremblay and Benner, 2009), indicated that the POM from the bloom was relatively fresh or unaltered, but was more rapidly degraded during sinking than the POM from the HNLC site (Table 3). These findings could explain the lower efficiency of carbon export at 100 m at the bloom sites A3-2 (5 %) and E-5 (11 %) than in HNLC waters (Station R-2, 34 %) (Planchon et al., 2014). Laurenceau et al. (2014) also found that export efficiencies (at 200 m) were negatively correlated to net primary productivity during the same sampling campaign.

In contrast to THAA yields, no consistent trend in mol% D-AA and DI values were observed with depth, probably because more intense degradation of bulk POM is required to be detectable with these markers (Davis et al., 2009; Bourgoin and Tremblay, 2010). Our data show that a large fraction of particulate AA is rapidly utilized in surface waters of the bloom. The AA that remain in the POM below the surface layer are probably in more refractory structures. These structures may be too recalcitrant to show significant change in AA composition (i.e., mol% D-AA and DI values) with depth. In addition, an apparent mismatch between DI values and the expected trend during degradation has been previously observed in the Southern Ocean and was attributed to the unusual AA composition of diatoms, the dominant source of POM (Ingalls et al., 2003).

BGD
11, 14097–14132, 2014

4.3 Origin and fate of DOM

Although an important fraction of the primary production is transferred to the DOM pool (e.g., 30–50 % as short lived labile DOM: Pomeroy et al., 2007; Obernosterer et al., 2008; Hansell, 2013), it was not possible to estimate the phytoplankton contribution to bulk DOC with the markers used in the present study. By contrast, the bacterial contribution to DOC was estimated using D-AA yields, indicating that 16.5–35 % of bulk DOC was of bacterial origin with no consistent trend with depth or location. These contributions were near 30 % in surface waters, and similar between Fe-fertilized waters and the HNLC site (Table 3). Similarly, DOC concentrations were not substantially different among sites (i.e., 3–4 µM greater in the bloom). Taken together, these results suggest that DOM production was counterbalanced by bacterial consumption (Christaki et al., 2014) of DOM from bacteria and other sources. The relatively constant bacterial contribution to DOC measured here (~ 30 %) or in the North Atlantic and North Pacific (~ 25 %, Kaiser and Benner, 2008) indicates that bacterial DOM has an average reactivity similar to bulk DOM and contributes to all DOM fractions, from labile to refractory DOM.

This study shows for the first time the contrasting fates of the DOM produced during natural iron fertilization and the DOM from an HNLC region (Table 3). The bloom site A3-2 clearly shows intense DOM alteration within the water column. At Station A3-2, all the molecular diagenetic markers (%DOC_{AA}, mol% D-AA, DI values) indicated that surface DOM was less altered than deep water DOM. In contrast, DOM in HNLC surface waters revealed a lower alteration state that did not change with depth (Table 3). The DOM produced during the bloom was thus more rapidly degraded and mineralized, and this pattern reflects well that observed for POM. Mixing of deep and surface water layers at Station A3-2 could explain the gradual character of the trends observed in profiles of DOM molecular markers at this location. Despite the fact that a water-column stratification was present during sampling, with a surface mixed layer of 153 m, Station A3-2 is located above the Kerguelen plateau which is surrounded by deeper areas

BGD
11, 14097–14132, 2014

and thus a more intense or frequent vertical mixing may occur. However, this probable mixing cannot explain why Station A3-2 had more altered DOM (and lower dissolved AA) than in the HNLC area even in deep waters.

A surprising finding of the present study is the lower total dissolved AA concentrations and yields in surface water DOM in the bloom sites as compared to HNLC waters. These differences were due to ~ 30 % more dissolved combined AA in HNLC waters. By contrast, free AA had higher concentrations and represented a greater proportion of dissolved AA at the bloom sites (13.5–23.6 % vs. 11.3 % at HNLC) which likely reflects the higher phytoplankton activity and associated DOM release mechanisms (Fuhrman, 1987; Sarmento et al., 2013).

We propose four possibilities that could explain the lower alteration state of DOM and the higher concentration of dissolved combined AA in less productive sites (i.e., stations R-2 and E-1) compared to the bloom sites (i.e., stations A3-2 and E-5). First, the higher quantities of labile DOM produced at the bloom sites could induce a priming effect (Bianchi, 2011). These large quantities of labile DOM (e.g., free AA) induce a strong microbial response (Christaki et al., 2014) and the energy gained through labile DOM may allow the degradation of more recalcitrant DOM including dissolved combined AA. This degradation was particularly marked within the water column of the bloom site A3-2. As a consequence, the DOM at the bloom sites appears more altered than the DOM from the HNLC site (Table 3). The higher concentration of more altered DOM in the bloom sites is consistent with the microbial carbon pump concept in which marine microbes transform labile DOM into refractory DOM (Jiao et al., 2011). Important inputs of labile DOM likely stimulate bacterial activity leading to more intense DOM degradation and production of more recalcitrant DOM. The more rapid degradation of the DOM from the bloom is consistent with a recent study in Arctic fjords (Osterholz et al., 2014). Their findings suggest that DOM produced during the spring/summer bloom is degraded in a few weeks by a specialized resident microbial community.

A second reason for the slower DOM degradation and the accumulation of combined dissolved AA in HNLC waters is an iron limitation for heterotrophic bacteria (Obernos-

BGD
11, 14097–14132, 2014

terer et al., 2014). Third, the DOM in HNLC waters can be involved in physicochemical processes (e.g., inter-molecular interactions, partial photooxidation) that protect DOM such as dissolved combined AA from microbial attack (Keil and Kirchman, 1994). Protection mechanisms may be too slow to significantly reduce the microbial degradation rate of the labile DOM produced during the bloom. A fourth explanation could be that HNLC waters produce DOM molecules, including ones that contain combined AA, that are more recalcitrant to degradation.

The first three explanations are associated with unfavorable conditions for DOM degradation in HNLC areas, namely low quantity of labile or priming DOM, iron limitation, and DOM protection. The last explanation implies that the DOM produced in the HNLC region is intrinsically more recalcitrant than the DOM produced during the bloom. Though the DOM from the HNLC site appears less degraded, the relative lability or recalcitrance of this DOM remains unknown. This notion of substrate quality "may only be valid in the context of the ambient environment" or conditions (Bianchi, 2011). Freshly produced and highly altered or old molecules can persist in unfavorable conditions, but be degraded in another environment.

5 Conclusions

Important differences in POM and DOM origins, compositions, and alterations were observed between the HNLC region and the areas where a phytoplankton bloom was induced by natural iron fertilization in the Southern Ocean. Phytoplankton cells represent an important fraction of POC (~ 45 %) in the surface waters at the bloom sites, while the bacterial total (cells and detritus) contribution was much lower (~ 15 %). Molecular indicators demonstrate that POM originating from the bloom was more rapidly degraded during sinking than the POM from the HNLC site. The fraction of the bloom POM that was transferred to DOM is unknown, but ~ 30 % of the DOM appears to come from bacteria. As for POM, the DOM from the bloom sites was involved in more intense degradation processes. In contrast, the DOM in HNLC waters was less altered and

BGD
11, 14097–14132, 2014

showed no significant alteration throughout the water column. The bloom induced by natural iron fertilization probably leads to favorable conditions (e.g., large quantities of labile OM) supporting high microbial activity (Christaki et al., 2014) and enhanced POM and DOM degradation. The more intense degradation in bloom sites reduces the carbon export efficiency and the net impact of such blooms on the global carbon budget. However, a higher microbial activity appears to also lead to a greater production of more recalcitrant DOM or a more active microbial carbon pump (Jiao et al., 2011).

Acknowledgements. We thank Louise Oriol and Karine Escoubeyrou for their help during sampling and analyses. This research was supported by the project KEOPS2 (ANR-10-Blanc-614, LEFE INSU), IPEV, the Natural Science and Engineering Research Council of Canada (NSERC). L. Tremblay received support from the UPMC during his sabbatical stay at the Laboratoire d'Océanographie Microbienne. We are grateful to the BIO2MAR platform (http://bio2mar.obs-banyuls.fr) for providing access to instrumentation.

References

Aminot, A. and Kérouel, R.: Dosage Automatique des Nutriments dans les Eaux Marines: Meìthodes en Flux Continu, Ifremer, France, 188 pp., 2007.

Asano, Y. and Lübbehüsen, T. L.: Enzymes acting on peptides containing d-amino acid, J. Biosci. Bioeng., 89, 295–306, 2000.

Benner, R.: Chemical composition and reactivity, in: Biogeochemistry of Marine Dissolved Organic Matter, edited by: Hansell, D. and Carlson, C., Academic Press, 59–90, 2002.

Benner, R. and Strom, M.: A critical-evaluation of the analytical blank associated with DOC measurements by high-temperature catalytic-oxidation, Mar. Chem., 41, 153–160, 1993.

Bianchi, T. S.: The role of terrestrially derived organic carbon in the coastal ocean: a changing paradigm and the priming effect, P. Natl. Acad. Sci. USA, 108, 19473–19481, 2011.

Blain, S., Carlotti, F., Christaki, U., Corbière, A., Durand, I., Ebersbach, F., Fuda, J., Garcia, N., Gerringa, L., Griffiths, B., Guigue, C., Quéguiner, B., Guillerm, C., Jacquet, S., Jeandel, C., Laan, P., Lefèvre, D., Lo Monaco, C., Malits, A., Mosseri, J., Obernosterer, I., Park, Y., Armand, L., Picheral, M., Pondaven, P., Remenyi, T., Sandroni, V., Sarthou, G., Savoye, N., Scouarnec, L., Souhaut, M., Thuiller, D., Timmermans, K., Belviso, S., Trull, T., Uitz, J., van

BGD
11, 14097–14132, 2014

Beek, P., Veldhuis, M., Vincent, D., Viollier, E., Vong, L., Wagener, T., Bombled, B., Bopp, L., Bowie, A., Brunet, C., and Brussaard, C.: Effect of natural iron fertilization on carbon sequestration in the Southern Ocean, Nature, 446, 1070–1074, 2007.

Blain, S., Capparos, J., Guéneuguès, A., Obernosterer, I., and Oriol, L.: Distributions and stoichiometry of dissolved nitrogen and phosphorus in the iron fertilized region near Kerguelen (Southern Ocean), Biogeosciences Discuss., 11, 9949–9977, doi:10.5194/bgd-11-9949-2014, 2014.

Bourgoin, L. and Tremblay, L.: Bacterial reworking of terrigenous and marine organic matter in estuarine water columns and sediments, Geochim. Cosmochim. Ac., 74, 5593–5609, 2010.

Bowie et al.: Iron budgets for three distinct biogeochemical sites around the Kerguelen Plateau (Southern Ocean) during the natural fertilization experiment KEOPS-2, Biogeosciences Discuss., in preparation, 2014.

Boyd, P. W., Jickells, T., Law, C. S., Blain, S., Boyle, E. A., Buesseler, K. O., Coale, K. H., Cullen, J. J., de Baar, H. J. W., Follows, M., Harvey, M., Lancelot, C., Levasseur, M., Owens, N. P. J., Pollard, R., Rivkin, R. B., Sarmiento, J., Schoemann, V., Smetacek, V., Takeda, S., Tsuda, A., Turner, S., and Watson, A. J.: Mesoscale iron enrichment experiments 1993–2005: synthesis and future directions, Science, 315, 612–617, 2007.

Brückner, H., Haasmann, S., Langer, M., Westhauser, T., Wittner, R., and Godel, H.: Liquid chromatographic determination of d- and l-amino acids by derivatization with o-phthaldialdehyde and chiral thiols, J. Chromatogr. A, 666, 259–273, 1994.

Christaki, U., Obernosterer, I., Van Wambeke, F., Veldhuis, M., Garcia, N., and Catala, P.: Microbial food web structure in a naturally iron-fertilized area in the Southern Ocean (Kerguelen Plateau), Deep-Sea Res. Pt. II, 55, 706–719, 2008.

Christaki, U., Lefèvre, D., Georges, C., Colombet, J., Catala, P., Courties, C., Sime-Ngando, T., Blain, S., and Obernosterer, I.: Microbial food web dynamics during spring phytoplankton blooms in the naturally iron-fertilized Kerguelen area (Southern Ocean), Biogeosciences Discuss., 11, 6985–7028, doi:10.5194/bgd-11-6985-2014, 2014.

Church, M. J., Hutchins, D. A., and Ducklow, H. W.: Limitation of bacterial growth by dissolved organic matter and iron in the Southern ocean, Appl. Environ. Microbi., 66, 455–466, 2000.

Cowie, G. and Hedges, J.: Sources and reactivities of amino-acids in a coastal marine environment, Limnol. Oceanogr., 37, 703–724, 1992.

Cowie, G. and Hedges, J.: Biochemical indicators of diagenetic alteration in natural organic matter mixtures, Nature, 369, 304–307, 1994.

BGD
11, 14097–14132, 2014

Dauwe, B., Middelburg, J. J., Herman, P. M. J., and Heip, C. H. R.: Linking diagenetic alteration of amino acids and bulk organic matter reactivity, Limnol. Oceanogr., 44, 1809–1814, 1999.
Davis, J., Kaiser, K., and Benner, R.: Amino acid and amino sugar yields and compositions as indicators of dissolved organic matter diagenesis, Org. Geochem., 40, 343–352, 2009.
Dittmar, T., Fitznar, H. P., and Kattner, G.: Origin and biogeochemical cycling of organic nitrogen in the eastern Arctic Ocean as evident from D- and L-amino acids, Geochim. Cosmochim. Ac., 65, 4103–4114, 2001.
Dittmar, T., Cherrier, J., and Ludwichowski, K.: The analysis of amino acids in seawater, in: Practical Guidelines for the Analysis of Seawater, edited by: Wurl, O., CRC Press, 67–77, 2009.
Ebersbach, F. and Trull, T.: Sinking particle properties from polyacrylamide gels during the KErguelen Ocean and Plateau compared Study (KEOPS): zooplankton control of carbon export in an area of persistent natural iron inputs in the Southern Ocean, Limnol. Oceanogr., 53, 212–224, 2008.
Escoubeyrou, K. and Tremblay, L.: Quantification of free, dissolved combined, particulate, and total amino acid enantiomers using simple sample preparation and more robust chromatographic procedures, Limnol. Oceanogr.-Meth., 12, 421–431, 2014.
Fuhrman, J.: Close coupling between release and uptake of dissolved free amino acids in seawater studied by an isotope dilution approach, Mar. Ecol.-Prog. Ser., 37, 45–52, 1987.
Fukuda, R., Ogawa, H., Nagata, T., and Koike, I.: Direct determination of carbon and nitrogen contents of natural bacterial assemblages in marine environments, Appl. Environ. Microb., 64, 3352–3358, 1998.
Gupta, L. and Kawahata, H.: Amino acid and hexosamine composition and flux of sinking particulate matter in the equatorial Pacific at 175 degrees E longitude, Deep-Sea Res. Pt. I, 47, 1937–1960, 2000.
Hansell, D.: Recalcitrant dissolved organic carbon fractions, Annu. Rev. Mar. Sci., 5, 421–445, 2013.
Ingalls, A. E., Lee, C., Wakeham, S. G., and Hedges, J. I.: The role of biominerals in the sinking flux and preservation of amino acids in the Southern Ocean along 170° W, Deep-Sea Res. Pt. II, 50, 713–738, 2003.
Ittekkot, V., Deuser, W., and Degens, E.: Seasonality in the fluxes of sugars, amino acids, and amino sugars to the deep ocean: Sargasso Sea, Deep-Sea Res., 31, 1057–1069, 1984.

BGD
11, 14097–14132, 2014

Jiao, N., Azam, F., and Sanders, S.: Microbial Carbon Pump in the Ocean, Sciences/AAAS, Washington, DC, 2011.
Kaiser, K. and Benner, R.: Hydrolysis-induced racemization of amino acids, Limnol. Oceanogr.-Meth., 3, 318–325, 2005.
Kaiser, K. and Benner, R.: Major bacterial contribution to the ocean reservoir of detrital organic carbon and nitrogen, Limnol. Oceanogr., 53, 99–112, 2008.
Kawasaki, N., Sohrin, R., Ogawa, H., Nagata, T., and Benner, R.: Bacterial carbon content and the living and detrital bacterial contributions to suspended particulate organic carbon in the North Pacific Ocean, Aquat. Microb. Ecol., 62, 165–176, 2011.
Keil, R. G. and Kirchman, D. L.: Abiotic transformation of labile protein to refractory protein in sea water, Mar. Chem., 45, 187–196, 1994.
Lasbleiz, M.: Dynamique nutritionnelle du phytoplancton, cycles biogéochimiques du carbone et des éléments biogènes associées (N,P,Si) et disponibilité du fer dans l'Océan Austral – programme KEOPS 2, PhD thesis, Aix Marseille Université, submitted, 2014.
Lasbleiz, M., Leblanc, K., Blain, S., Ras, J., Cornet-Barthaux, V., Hélias Nunige, S., and Quéguiner, B.: Pigments, elemental composition (C, N, P, Si) and stoichiometry of particulate matter, in the naturally iron fertilized region of Kerguelen in the Southern Ocean, Biogeosciences Discuss., in press, 2014.
Laurenceau, E. C., Trull, T. W., Davies, D. M., Bray, S. G., Doran, J., Planchon, F., Carlotti, F., Jouandet, M.-P., Cavagna, A.-J., Waite, A. M., and Blain, S.: The relative importance of phytoplankton aggregates and zooplankton fecal pellets to carbon export: insights from free-drifting sediment trap deployments in naturally iron-fertilised waters near the Kerguelen plateau, Biogeosciences Discuss., 11, 13623–13673, doi:10.5194/bgd-11-13623-2014, 2014.
Le Quéré, C., Rodenbeck, C., Buitenhuis, E. T., Conway, T. J., Langenfelds, R., Gomez, A., Labuschagne, C., Ramonet, M., Nakazawa, T., Metzl, N., Gillett, N., and Heimann, M.: Saturation of the southern ocean CO_2 sink due to recent climate change, Science, 316, 1735–1738, 2007.
Lee, C., Wakeham, S. G., and I. Hedges, J.: Composition and flux of particulate amino acids and chloropigments in equatorial Pacific seawater and sediments, Deep-Sea Res. Pt. I, 47, 1535–1568, 2000.
Nagata, T., Meon, B., and Kirchman, D.: Microbial degradation of peptidoglycan in seawater, Limnol. Oceanogr., 48, 745–754, 2003.

BGD
11, 14097–14132, 2014

Obernosterer, I., Christaki, U., Lefèvre, D., Catala, P., Van Wambeke, F., and Lebaron, P.: Rapid bacterial mineralization of organic carbon produced during a phytoplankton bloom induced by natural iron fertilization in the Southern Ocean, Deep-Sea Res. Pt. II, 55, 777–789, 2008.
Obernosterer, I., Fourquez, M., and Blain, S.: Iron and carbon limitation of heterotrophic bacteria in the naturally iron fertilized Southern Ocean, Biogeosciences Discuss., in preparation, 2014.
Osterholz, H., Dittmar, T., and Niggemann, J.: Molecular evidence for rapid dissolved organic matter turnover in Arctic fjords, Mar. Chem., 160, 1–10, 2014.
Peter, S., Shen, Y., Kaiser, K., Benner, R., and Durisch-Kaiser, E.: Bioavailability and diagenetic state of dissolved organic matter in riparian groundwater, J. Geophys. Res.-Biogeo., 117, G04006, doi:10.1029/2012JG002072, 2012.
Planchon, F., Ballas, D., Cavagna, A. J., Van Der Merwe, P., Bowie, A., Trull, T., Laurenceau, E., Davis, D., and Dehairs, F.: Carbon export in the naturally iron fertilized Kerguelen area of the Southern Ocean using ^{234}Th-based approach, Biogeosciences Discuss., in preparation, 2014.
Pomeroy, L., Williams, P., Azam, F., and Hobbie, J.: The Microbial Loop, Oceanography, 20, 28–33, 2007.
Ras, J., Claustre, H., and Uitz, J.: Spatial variability of phytoplankton pigment distributions in the Subtropical South Pacific Ocean: comparison between in situ and predicted data, Biogeosciences, 5, 353–369, doi:10.5194/bg-5-353-2008, 2008.
Salter, I., Kemp, A., Lampitt, R., and Gledhill, M.: The association between biogenic and inorganic minerals and the amino acid composition of settling particles, Limnol. Oceanogr., 55, 2207–2218, 2010.
Sarmento, H., Romera-Castillo, C., Lindh, M., Pinhassi, J., Sala, M., Gasol, J., Marrase, C., and Taylor, G.: Phytoplankton species-specific release of dissolved free amino acids and their selective consumption by bacteria, Limnol. Oceanogr., 58, 1123–1135, 2013.
Sathyendranath, S., Stuart, V., Nair, A., Oka, K., Nakane, T., Bouman, H., Forget, M. H., Maass, H., and Platt, T.: Carbon-to-chlorophyll ratio and growth rate of phytoplankton in the sea, Mar. Ecol.-Prog. Ser., 383, 73–84, 2009.
Savoye, N., Trull, T. W., Jacquet, S. H. M., Navez, J., and Dehairs, F.: ^{234}Th-based export fluxes during a natural iron fertilization experiment in the Southern Ocean (KEOPS), Deep-Sea Res. Pt. II, 55, 841–855, 2008.

BGD
11, 14097–14132, 2014

Silver, M. W. and Gowing, M. M.: The “particle” flux: origins and biological components, Prog. Oceanogr., 26, 75–113, 1991.
Tremblay, L. and Benner, R.: Microbial contributions to N-immobilization and organic matter preservation in decaying plant detritus, Geochim. Cosmochim. Ac., 70, 133–146, 2006.
Tremblay, L. and Benner, R.: Organic matter diagenesis and bacterial contributions to detrital carbon and nitrogen in the Amazon River system, Limnol. Oceanogr., 54, 681–691, 2009.
Van Heukelem, L. and Thomas, C. S.: Computer-assisted high-performance liquid chromatography method development with applications to the isolation and analysis of phytoplankton pigments, J. Chromatogr. A, 910, 31–49, 2001.
White, D. S. and Howes, B. L.: Nitrogen incorporation into decomposing litter of Spartina alterniflora, Limnol. Oceanogr., 39, 133–140, 1994.
Zubkov, M. V., Holland, R. J., Burkill, P. H., Croudace, I. W., and Warwick, P. E.: Microbial abundance, activity and iron uptake in vicinity of the Crozet Isles in November 2004–January 2005, Deep-Sea Res. Pt. II, 54, 2126–2137, 2007.

BGD
11, 14097–14132, 2014

Table 1. Sampling sites, chlorophyll *a* (Chl *a*) concentrations, particulate and dissolved organic carbon (POC, DOC) and nitrogen (PON, DON) concentrations, and amino acid (AA) concentrations in particulate and dissolved (including free AA) phases.

Stations	Coordinates Latitude °S	Longitude °E	Depth (m)	[Chl *a*] ($\mu g\,L^{-1}$)[a]	[POC] (μM)[a]	[DOC] (μM)	[PON] (μM)[a]	[DON] (μM)[b]	[AA] partic.[c] (nM)	dissolv.[d] (nM)	free (nM)	free AA[e] (%)
R-2	50.383	66.683	40	0.32	7.8	48	0.8	6.0	162	335	38	11.3
(HNLC)[f]			70	0.27	nd	47	nd	6.1	262	216	nd	
27 Oct 2011[g]			100	0.23	5.2	48	0.7	6.9	498	276	nd	
			200	0.02	2.9	47	0.3	nd	45	173	nd	
			300	nd	nd	45	nd	nd	23	198	nd	
			500	nd	1.5	44	0.1	nd	77	186	nd	
			900	nd	1.6	45	0.1	nd	92	192	11	5.7
			1300	nd	nd	44	nd	nd	33	151	nd	
A3-2	50.617	72.050	40	1.7	14.8	52	2.8	6.0	821	277	52	18.8
17 Nov 2011[g]			70	2.1	14.3	51	2.6	5.1	716	292	69	23.6
			110	2.4	13.9	50	2.6	3.9	656	237	nd	
			150	1.4	10.8	48	2.1	5.3	400	173	nd	
			210	0.15	3.5	47	0.4	3.9	44	144	10	6.9
			300	0.05	2.0	48	0.3	2.7	22	128	nd	
E-5	48.400	71.884	25	1.2	11.0	48	2.2	6.5	539	208	28	13.5
18 Nov 2011[g]			70	0.95	9.1	47	2.2	7.0	333	234	nd	
			110	0.36	nd	47	0.6	6.8	71	160	nd	
			200	0.12	3.5	46	0.3	6.9	45	191	6	3.1
			350	nd	3.0	45	0.2	nd	27	146	nd	
E-1	48.450	72.183	20	0.99	7.7	49	1.3	4.8	223	406	nd	
30 Oct 2011[g]			40	0.96	8.9	49	1.6	5.0	486	352	nd	
			70	0.86	4.5	47	1.0	5.2	124	495	nd	
			120	0.78	6.5	46	1.2	6.4	387	289	nd	
			200	0.07	5.1	45	1.0	nd	203	314	nd	
			500	nd	1.6	45	0.1	nd	nd	383	nd	
			1300	nd	nd	45	nd	nd	44	199	nd	
TEW-2	48.884	70.650	15	1.8	9.3	47	1.5	7.4	627	413	37	9.0
(shelf)			30	1.4	5.7	46	1.0	7.1	338	489	nd	
31 Oct 2011[g]			62	0.6	6.4	45	0.7	7.6	205	403	11	2.7

[a] Data are from Lasbleiz et al. (2014).
[b] Data are from Blain et al. (2014).
[c] Particulate AA = total hydrolysable amino acids (THAA).
[d] Dissolved AA = dissolved combined and free amino acids.
[e] % free amino acids vs. dissolved AA.
[f] High-nutrient low chlorophyll.
[g] Dates of sampling.
nd = not determined.

BGD
11, 14097–14132, 2014

Table 2. Yields of D-amino acids (D-AA) in particulate and dissolved fractions along with average yields measured in cultured bacteria and bacterial dissolved organic matter.

Stations	Depth (m)	D-Asx[a]	D-Glx[b]	D-Ala[c]	D-Asx	D-Glx	D-Ala
		nmol (mg POC)$^{-1}$			nmol (mg DOC)$^{-1}$		
R-2	40	10.2	2.83	13.9	5.31	1.77	10.6
(HNLC)	70	nd	nd	nd	6.09	1.59	9.75
27 Oct 2011	100	7.06	6.36	68.8	6.52	1.81	4.70
	200	31.7	18.1	53.7	4.27	0.81	7.17
	300	nd	nd	nd	6.58	1.63	11.3
	500	nd	nd	nd	3.80	1.06	7.69
	900	5.48	8.22	nd	4.85	1.84	10.5
	1300	nd	nd	nd	5.30	1.82	9.53
A3-2	40	13.5	9.33	5.34	6.36	2.61	11.0
17 Nov 2011	70	9.80	8.99	2.17	6.88	2.56	12.1
	110	6.12	7.65	2.62	7.29	2.63	11.9
	150	7.30	6.25	6.77	6.59	2.62	11.0
	210	nd	2.40	7.51	6.88	2.61	11.6
	300	nd	6.57	nd	6.80	2.09	10.5
E-5	25	14.8	10.5	4.25	7.44	3.24	13.5
18 Nov 2011	70	9.67	4.37	10.4	8.14	3.38	12.9
	110	nd	nd	nd	7.32	2.87	13.0
	200	7.79	1.91	10.8	6.95	2.50	13.0
	350	2.13	0.55	nd	6.82	2.73	14.1
E-1	20	1.70	7.13	nd	5.64	2.45	12.1
30 Oct 2011	40	5.27	4.62	14.0	5.39	2.47	11.2
	70	nd	2.70	4.34	7.47	2.92	11.4
	120	nd	7.09	nd	6.51	2.44	11.3
	200	nd	2.17	nd	2.69	2.44	9.94
	500	nd	nd	nd	1.94	1.88	5.63
	1300	8.39	nd	nd	2.63	2.25	8.17
TEW-2	15	nd	2.85	nd	8.39	4.13	14.7
31 Oct 2011	30	21.3	14.3	nd	8.46	4.24	15.8
	62	9.26	2.74	nd	8.12	4.10	16.0
Bacteria[d]		15 (22)	48 (26)	50 (19)	24 (3)	17 (7)	35 (7)

[a, b, c] D-aspartic acid or D-asparagine, D-glutamic acid or D-glutamine, and D-alanine, respectively.
[d] From Kaiser and Benner (2008). POC-normalized values are averages from 3 phototrophic and 5 heterotrophic marine bacteria assuming 20 % phototrophic and 80 % heterotrophic. DOC-normalized values are averages measured in 3 DOM samples freshly produced by bacteria. Values in parentheses are standard deviations.
nd = not determined or below detection (for POC or D-AA measurements).

BGD
11, 14097–14132, 2014

Table 3. Summary of the characteristics of particulate and dissolved organic matter (POM and DOM) in high-nutrient low-chlorophyll (HNLC) waters (Station R-2) and at the bloom site above the Kerguelen Plateau (Station A3-2). Surface refers to 10–90 m depth layer and deep refers to 210–300 m depth. Contributions to POM and DOM are average values given as percent of bulk organic carbon.

Depth	Parameters	POM HNLC	POM Bloom	DOM HNLC	DOM Bloom
Surface					
	Phytoplankton				
	diatom cells[a]	5 %	44 %	nd	nd
	total cells[b]	14 %	45 %	nd	nd
	Bacteria				
	cells [c]	5 %	3 %	nd	nd
	total [d]	> 15 %[g]	15 %	30 %	30 %
	Alteration state	high	low	low	med
	Alterations with depth[e]	med	high	low	high
Deep					
	Phytoplankton				
	total cells [b]	2 %	8 %	nd	nd
	phytodetritus [f]	34 %	41 %	nd	nd
	Bacteria				
	cells [c]	7 %	10 %	nd	nd
	total[d]	> 15 %[g]	15 %	25 %	30 %
	Alteration state	high	high	med	high

[a] From microscopic counts and biovolume determination (Lasbleiz, 2014).
[b] Total cells assuming that phytoplankton cells have 40 times more carbon than chlorophyll *a* (Sathyendranath et al., 2009).
[c] From cell counts of autotrophic and heterotrophic bacteria and conversion factors (Christaki et al., 2014).
[d] Total bacterial contribution estimated from D-AA yields (see text), for POC it includes living cells and cell fragments or detritus.
[e] Alterations promoted by different organic matter inputs or environmental conditions (see text).
[f] Estimated based on direct observation of sinking particles defined as phytodetrital aggregates (Laurenceau et al., 2014).
[g] Estimates were inconsistent but generally > 15 % (see text).
nd = not determined
med = medium

BGD
11, 14097–14132, 2014

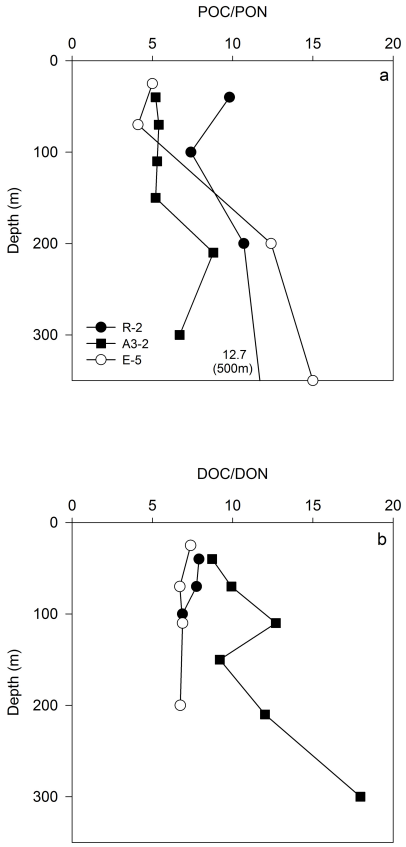

Figure 1. Carbon to nitrogen atomic ratios in the: **(a)** particulate and **(b)** dissolved fractions for three representative stations (R-2, A3-2, E-5) at 0–350 m depth. The value close to Station R-2 profile is the next data point at 500 m. Ratios cannot be quantified at certain depths because elementary data were not available (Table 1).

BGD
11, 14097–14132, 2014

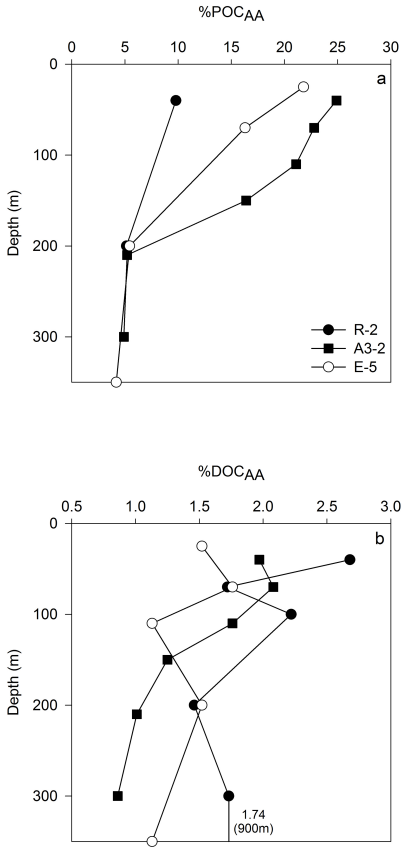

Figure 2. Proportion of: **(a)** particulate and **(b)** dissolved organic carbon quantified as amino acids (%POC_{AA} and % DOC_{AA}) for three representative stations (R-2, A3-2, E-5) at 0–350 m depth. The value close to Station R-2 profile is the next data point at 900 m.

BGD
11, 14097–14132, 2014

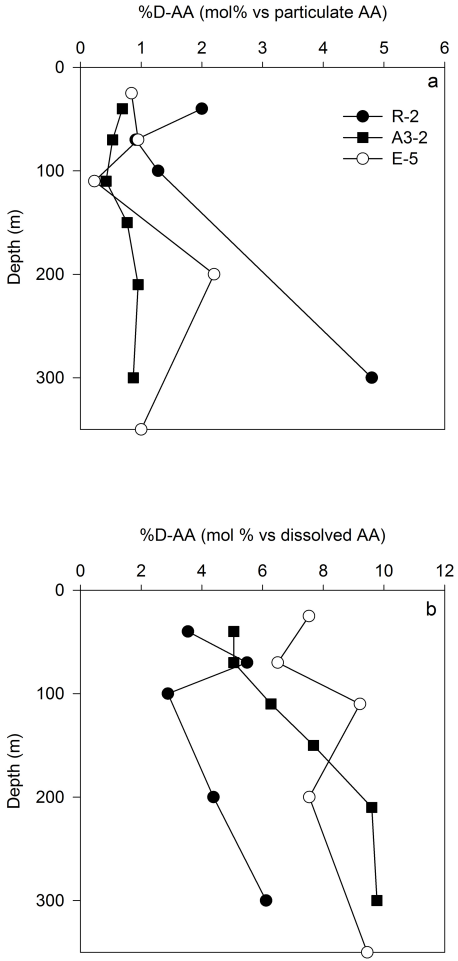

Figure 3. Proportion of D-amino acids (%D-AA) vs. total amino acids (AA) in the: **(a)** particulate and **(b)** dissolved fractions for three representative stations (R-2, A3-2, E-5) at 0–350 m depth.

BGD
11, 14097–14132, 2014

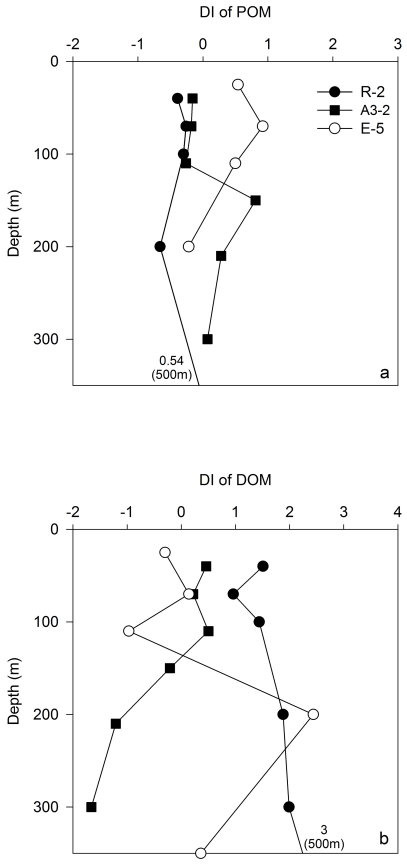

Figure 4. Degradation index (DI) of: **(a)** particulate organic matter (POM, Dauwe et al., 1999) and **(b)** dissolved organic matter (DOM, Peter et al., 2012) calculated for three representative stations (R-2, A3-2, E-5) at 0–350 m depth. Values close to Station R-2 profiles are the next data point at 500 m.

BGD
11, 14097–14132, 2014

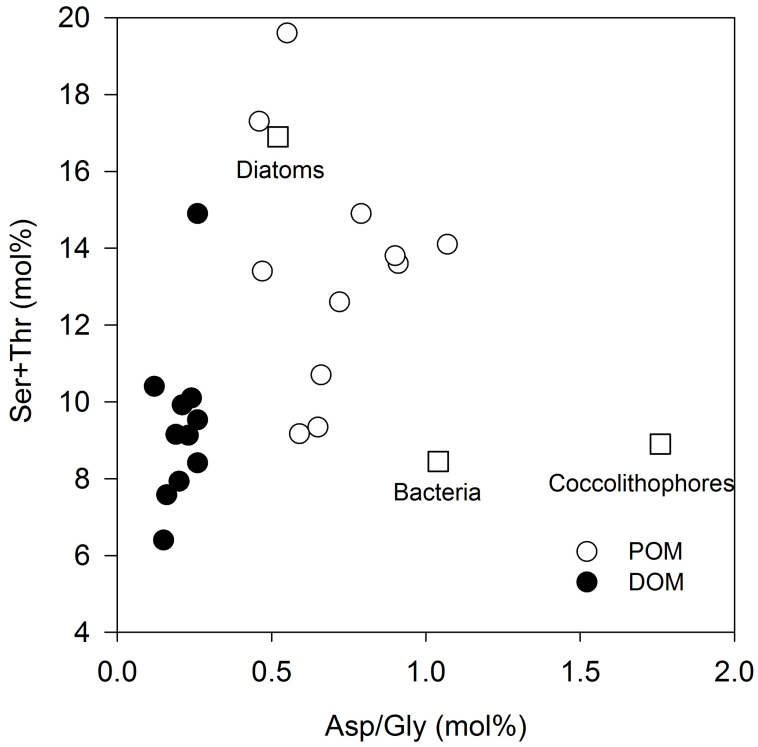

Figure 5. Molar contribution of serine + threonine (Ser + Thr) vs. the molar ratio of aspartic acid and glycine (Asp/Gly) in the particulate and dissolved organic matter (POM and DOM) of stations A3-2 and E-5. Average values for diatoms, coccolithophores, and bacteria are based on Muller et al. (1986) and Cowie and Hedges (1992).

BGD
11, 14097–14132, 2014

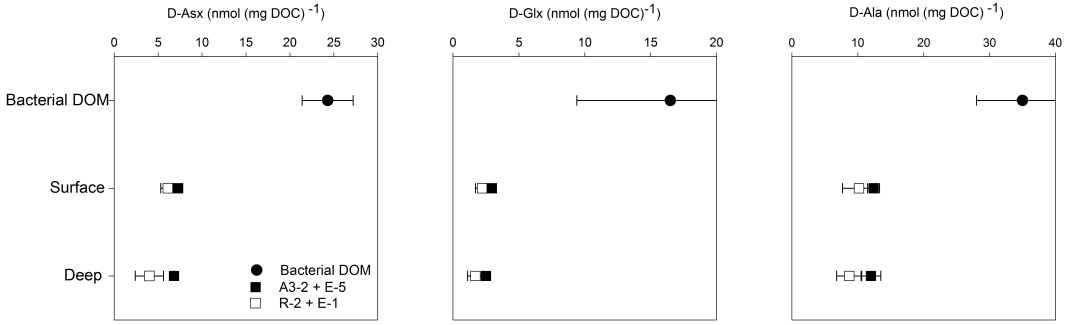

Figure 6. Average C-normalized yields of D-aspartic acid or D-asparagine (D-Asx), D-glutamic acid or D-glutamine (D-Glx), and D-alanine (D-Ala) in bacterial dissolved organic matter (Bacterial DOM, Kaiser and Benner 2008) and DOM from surface (0–120 m) and deep waters (> 120 m) at stations impacted (A3-2 + E-5) or not (R-2 + E-1) by the bloom. Error bars represent standard deviations.

BGD
11, 14097–14132, 2014